

Ground-state selection via many-body superradiant decay

Wai-Keong Mok ^{1,*}, Stuart J. Masson ², Dan M. Stamper-Kurn ^{3,4,5}, Tanya Zelevinsky ², and Ana Asenjo-Garcia ^{2,†}¹*Institute for Quantum Information and Matter, California Institute of Technology, Pasadena, California 91125, USA*²*Department of Physics, Columbia University, New York, New York 10027, USA*³*Department of Physics, University of California, Berkeley, California 94720, USA*⁴*Challenge Institute for Quantum Computation, University of California, Berkeley, California 94720, USA*⁵*Materials Sciences Division, Lawrence Berkeley National Laboratory, Berkeley, California 94720, USA* (Received 11 July 2024; revised 10 January 2025; accepted 12 February 2025; published 14 April 2025)

For a single particle, relaxation into different ground states is governed by fixed branching ratios determined by the transition matrix element and the environment. Here, we show that in many-body open quantum systems the occupation probability of one ground state can be boosted well beyond what is dictated by single-particle branching ratios. Despite the competition, interactions suppress all but the dominant decay transition, leading to a “winner takes all” dynamic where the system primarily settles into the dominant ground state. We prove that, in the presence of permutation symmetry, this problem is exactly solvable for any number of competing channels. Additionally, we develop an approximate model for the dynamics by mapping the evolution onto a fluid continuity equation, and analytically demonstrate that the dominant transition ratio converges to unity as a power law with increasing system size, for any branching ratios. This near-deterministic preparation of the dominant ground state has broad applicability. As an example, we discuss a protocol for molecular photoassociation where collective dynamics effectively acts as a catalyst, amplifying the yield in a specific final state. Our results open different avenues for many-body strategies in the preparation and control of quantum systems.

DOI: [10.1103/PhysRevResearch.7.L022015](https://doi.org/10.1103/PhysRevResearch.7.L022015)

The suppression of decay pathways into undesired quantum states is crucial for the control and manipulation of open quantum systems. Simplified theoretical models often rely on “closed” transitions where the excited state decays predominantly to a specific ground state. However, in practice, real-world emitters rarely adhere to the idealized paradigm of two-level systems. For instance, highly excited atomic states (such as Rydberg states) have many lower-energy states accessible by spontaneous emission [1]. In photochemistry, the decay to a single ground state is often inefficient due to numerous competing pathways arising from electronic, vibrational, and rotational degrees of freedom [2,3]. Solid-state emitters (such as color centers or dye molecules) also suffer from parasitic decay from phonon sidebands [4,5]. Achieving closed transitions in experiments is challenging and often involves isolating two-level systems from more complex internal structures or employing repumping techniques to redirect population back into the desired states. However, these approaches are inherently limited by the natural single-particle branching ratios of the transitions.

The natural branching ratios and dynamics of decay can, in fact, be modified by engineering the quantum system and its

environment. One common approach is to tailor the dielectric environment by placing emitters within optical cavities [6], waveguides [7,8], or other photonic structures [9,10] such that the desired decay channel is Purcell enhanced. Numerical studies with multilevel atoms [11–14] and molecules [15] have suggested collective emission as an alternative to circumvent limitations from single-particle branching ratios. These proposals rely on many-body transient superradiance [16,17], a phenomenon characterized by avalanchelike behavior [18–20] where decay into a given ground state enhances the probability of subsequent emission into that same state. This process effectively steers the emitters towards a specific ground state. A comprehensive analytical treatment of this physics remains lacking, which is critical for understanding and exploiting its potential.

We term the phenomenon in which correlated decay suppresses all but the most dominant emission path as *ground-state selection*. As shown in Fig. 1(a), we consider an ensemble of emitters coupled to a reservoir. The emitters have multiple decay channels, each leading to different final states. Each decay channel can be collectively enhanced by many-body correlations that emerge dynamically, leading to competition between them, effectively quenching the subdominant channels. We find approximate steady-state solutions for the populations of the different ground states by modeling the quantum dynamics through a continuity equation for a fluid. We prove that, despite the competition, the population density of the dominant ground state exhibits a power-law convergence to unity for any branching ratio, with the power-law exponent characterized by the ratio between dominant and subdominant decay rates. This is supported by

*Contact author: darielmok@caltech.edu†Contact author: ana.asenjo@columbia.edu

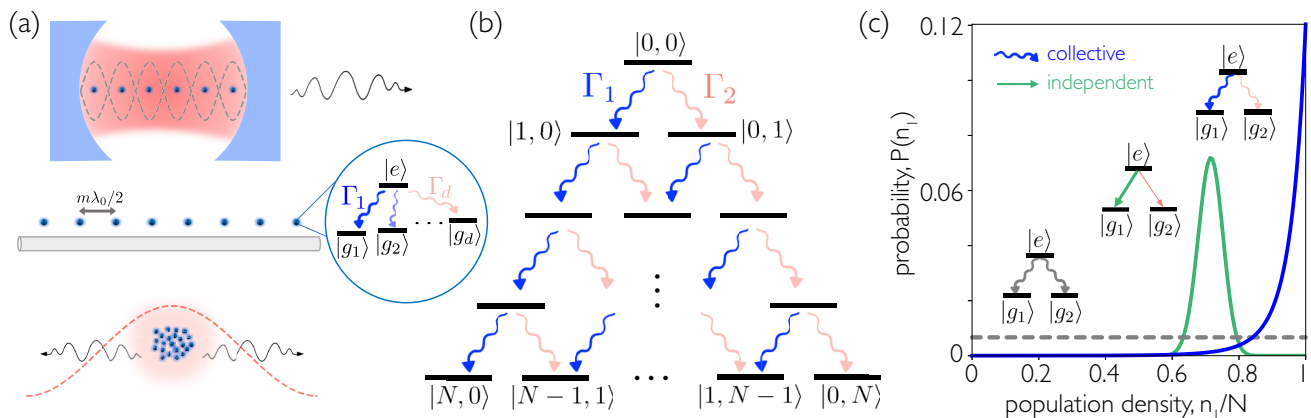


FIG. 1. Ground-state selection due to collective decay in multilevel systems. (a) N multilevel emitters with d ground states and a single excited state decay collectively to an environment (at rates $\Gamma_1, \dots, \Gamma_d$), such as a “bad” cavity, a waveguide in the “mirror configuration” (where the relative distance between the emitters is a half-integer multiple of the resonance wavelength λ_0) or free space (for the latter, a dense ensemble of subwavelength volume is required to preserve permutational symmetry). (b) Dissipative dynamics can be modeled as a random walk between permutationally symmetric ground states ($d = 2$ depicted), labeled by $|n_1, \dots, n_d\rangle$, where n_μ denotes the population of the ground state $|g_\mu\rangle$. (c) Marginal probability distribution $P(n_1) = \sum_{n_2} P(n_1, n_2)$ for the population density of the ground state $|g_1\rangle$, for $N = 150$ and $d = 2$ in the steady state, after complete depletion of the fully inverted initial state. The distributions for collective decay with $r_2 = 1$ (gray), and collective decay with $r_2 = 0.5$ (blue) are obtained via numerical simulations of Eq. (2). The binomial distribution is plotted for independent decay with $r_2 = 0.5$ (green).

a rigorous analysis of the exact steady-state solution. Our analytical treatment provides physical insights on the phenomenon beyond the numerical observations in Refs. [12–14]. We apply our framework to the problem of photochemistry, where suboptimal branching ratios limit the effectiveness of molecule creation, direct laser cooling [21], and optical imaging. Specifically, in molecular photoassociation of strontium dimers, we demonstrate that ground-state selection greatly enhances sample purity.

We consider an (undriven) ensemble of N identical emitters. Each emitter has a level structure consisting of a single excited state $|e\rangle_i$ and d ground states labeled $|g_\mu\rangle_i$, with $\mu \in \{1, \dots, d\}$ and $i \in \{1, \dots, N\}$. The level structure describes natural emitters including atoms, trapped ions, and color centers. The emitters are symmetrically coupled to a Markovian environment, with separate couplings for each transition $|e\rangle \rightarrow |g_\mu\rangle$. Physically, this can be realized by coupling the emitters to near-resonant cavity modes (in the “bad cavity” or “weak-coupling” limit, and placing the emitters in locations where they couple with the same strength to the cavity mode), to a single-mode waveguide in the “mirror configuration” (where the emitters are separated by a half-integer multiple of the wavelength [22,23]), or via free-space interactions in a dense ensemble of subwavelength volume, as depicted in Fig. 1(a). We assume that photons from different transitions can be resolved either by polarization or frequency (for the waveguide configuration, we assume that the transition frequencies are approximately equal to fulfill the mirror condition). The system dynamics is modeled by the master equation

$$\dot{\rho} = -i \left[\sum_{\mu=1}^d \chi_\mu \hat{A}_\mu^\dagger \hat{A}_\mu, \rho \right] + \sum_{\mu=1}^d \Gamma_\mu \mathcal{D}[\hat{A}_\mu] \rho, \quad (1)$$

where χ_μ are the coherent interaction rates, $\hat{A}_\mu = \sum_{i=1}^N (|g_\mu\rangle \langle e|)_i$ is the collective lowering operator on the

transition $|e\rangle \rightarrow |g_\mu\rangle$, and $\mathcal{D}[\hat{A}] \rho \equiv \hat{A} \rho \hat{A}^\dagger - \{\hat{A}^\dagger \hat{A}, \rho\} / 2$. Collective dissipation occurs with rates Γ_μ (identical to the single-emitter ones), and we assume the ordering $\Gamma_1 \geq \Gamma_2 \geq \dots \geq \Gamma_d$, such that Γ_1 is the dominant decay rate. For convenience, we denote the ratio between dominant and subdominant decay rates as $r_\mu \equiv \Gamma_\mu / \Gamma_1$. Our model also encompasses a more general scenario where some of the transitions are indistinguishable, such that d is the number of distinguishable channels.

Dynamical evolution can be understood as a random walk in the subspace of permutationally symmetric states, as shown in Fig. 1(b). Since Eq. (1) preserves permutation symmetry, basis states $|n_1, \dots, n_d\rangle$ are fully described by occupation numbers, where n_μ is the population of $|g_\mu\rangle$. These are typically entangled, as they consist of a symmetric superposition of excitations over N particles. The population of the excited state is $n_e = N - \sum_\mu n_\mu$, with $n_e = 0$ in the final steady state. Employing the ansatz $\rho = \sum_{\{n_\mu\}} P_{n_1, \dots, n_d} |n_1, \dots, n_d\rangle \langle n_1, \dots, n_d|$, Eq. (1) reduces to a rate equation [see Supplemental Material (SM) [24]]

$$\begin{aligned} \dot{P}_{n_1, \dots, n_d} = & - \left(N - \sum_{v=1}^d n_v \right) \sum_{\mu=1}^d \Gamma_\mu (n_\mu + 1) P_{n_1, \dots, n_\mu, \dots, n_d} \\ & + \left(N - \sum_{v=1}^d n_v + 1 \right) \sum_{\mu=1}^d \Gamma_\mu n_\mu P_{n_1, \dots, n_\mu-1, \dots, n_d} \end{aligned} \quad (2)$$

for the probabilities P_{n_1, \dots, n_d} of occupying the state $|n_1, \dots, n_d\rangle$. This ansatz is justified even if there are coherences in the initial state (i.e., off-diagonal terms in the density matrix), since they are decoupled and hence do not affect population dynamics. While the rate equation holds for any permutationally symmetric initial state, below we choose the fully inverted state (i.e., $|e\rangle^{\otimes N}$).

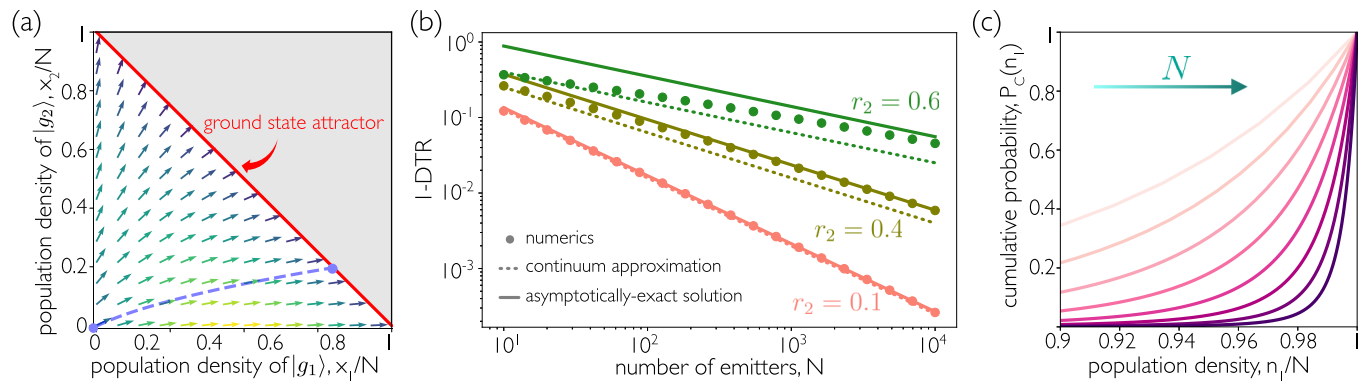


FIG. 2. (a) Velocity vector field of the continuum model for $r_2 = 0.5$ and $N = 10$. The dashed line represents the flow trajectory in the single-particle approximation starting from the fully excited state $(x_1, x_2) = (0, 0)$, where $x_{1(2)}$ denotes the population of $|g_{1(2)}\rangle$. Darker color indicates lower velocity. The red solid line shows the neutrally stable ground-state attractor. The unphysical region (where the ground-state population is larger than N) is shown in gray. (b) Population density outside the dominant ground state [1 - dominant transition ratio (DTR)] against number of emitters N , for various decay ratios $r_2 = \Gamma_2/\Gamma_1$. The points are obtained from numerically solving the rate equation (2), while the dotted lines denote the approximate formula (9). Solid lines denote the exact asymptotic solution (10). (c) Cumulative distribution (i.e., total probability of the dominant ground-state population being at most n_1) $P_c(n_1) = \sum_{n'_1=0}^{n_1} P(n'_1)$. Data obtained from numerical simulation of the rate equation (2), with $r_2 = 0.4$. Darker colors indicate larger number of emitters, with $61 \leq N \leq 10^4$. All plots are made for $d = 2$ ground states.

Although Eq. (2) can be efficiently simulated, it is nontrivial to obtain the steady state analytically. Moreover, the steady state is highly nonunique, since any combination of emitters in any ground state is a possible steady state. The trivial case of just one collective decay channel ($d = 1$) reduces to the problem of Dicke superradiance [16,17]. We instead focus on the problem of multiple competing transitions.

We quantify ground-state selection by the dominant transition ratio (DTR), defined as the mean population density of the dominant ground state in the steady state, i.e.,

$$\text{DTR} = \frac{\bar{n}_1}{N}, \quad (3)$$

where \bar{n}_1 is the mean number of emitters in $|g_1\rangle$ as $t \rightarrow \infty$. For independent emitters, the marginal probability distribution $P(n_1) = \sum_{n_2, \dots, n_d} P_{n_1, \dots, n_d}$ for the dominant ground state is a binomial distribution whose average (normalized by N) is the DTR $= (1 + \sum_{\mu>1} r_\mu)^{-1}$, determined solely by the decay ratios and independent of N [see Fig. 1(c)]. Below, we prove that the DTR always converges to 1 as $N \rightarrow \infty$ for any number of collective decay channels, assuming $\Gamma_1 > \Gamma_{\mu>1}$. This effect can be attributed to the superradiant enhancement, which amplifies the dominant transition relative to all subdominant transitions. If $\Gamma_1 = \Gamma_2 = \dots = \Gamma_d$, one obtains a uniform distribution for P_{n_1, \dots, n_d} [13], as shown in Fig. 1(c).

To gain analytical insights from the rate equation, we transform it into a continuity equation of a fluid that flows in Euclidean space. In the limit of large N , we make the continuum approximation [25] by setting $n_\mu \rightarrow x_\mu$, $\vec{x} = (x_1 \dots x_d)^T \in \mathbb{R}_+^d$, and $f(n_1, \dots, n_\mu, \dots, n_d) - f(n_1, \dots, n_\mu - 1, \dots, n_d) \rightarrow \frac{\partial}{\partial x_\mu} f(\vec{x})$ for an arbitrary differentiable function f . The rate equation is then approximated by the continuity equation

$$\frac{\partial}{\partial t} P(\vec{x}, t) = -\nabla \cdot [\vec{v}(\vec{x})P(\vec{x}, t)], \quad (4)$$

which describes a fluid flow in \mathbb{R}_+^d , governed by the position-dependent velocity field $\vec{v}(\vec{x})$ with the μ th component,

$$v_\mu(\vec{x}) = \Gamma_\mu \left(N - \sum_{\nu=1}^d x_\nu \right) (x_\mu + 1). \quad (5)$$

The flow comes to a stop as $\sum_\nu x_\nu \rightarrow N$, which physically corresponds to the system approaching its steady state, where no excited-state population remains. The velocity field is illustrated for $d = 2$ in Fig. 2(a). The fully excited initial state corresponds to the origin of \mathbb{R}_+^d . Due to the nonuniqueness of the steady state, it is not sufficient to simply solve for $\partial_t P = 0$.

Solving Eq. (4) analytically for arbitrary times is a formidable task. Instead, we employ a single-particle approximation where the fluid is idealized as a point particle initialized at the origin, with velocity dynamics $d\vec{x}/dt = \vec{v}(\vec{x})$. This reduces the partial differential equation in Eq. (4) to a coupled system of d ordinary differential equations. Dividing the components of $\vec{v}(\vec{x})$, we readily find

$$\frac{dx_\mu}{dx_\nu} = \frac{\Gamma_\mu x_\mu + 1}{\Gamma_\nu x_\nu + 1} \quad (6)$$

for any pair of $\mu, \nu \in \{1, \dots, d\}$. Integrating the above expression yields

$$(x_\mu + 1)^{\Gamma_\nu} = (x_\nu + 1)^{\Gamma_\mu}. \quad (7)$$

The $d - 1$ independent equations of the form (7) define the particle trajectory in \mathbb{R}_+^d starting from the origin. Generalizing Eq. (7) to other permutationally symmetric initial states is straightforward (see SM [24]).

The steady-state solution has a geometrical interpretation as the intersection between the particle trajectory and the hyperplane $\sum_{\mu=1}^d x_\mu = N$. To find an asymptotic solution, we assume that $x_\mu \gg 1$. The trajectory is then described by a simpler set of equations $x_\mu^{\Gamma_\nu} = x_\nu^{\Gamma_\mu}$. The constraint $\sum_{\mu=1}^d x_\mu = N$ can then be rewritten as $\sum_{\mu=1}^d x_\mu^{\Gamma_\mu/\Gamma_d} = N$. For simplicity,

we consider the nondegenerate case where all Γ_μ are distinct (see SM [24] for the degenerate case). Using the method of dominant balance [26] we obtain $x_d \approx N^{r_d}$, valid in the regime $1 \ll N^{r_d} \ll N$. In the regime $1 \ll N^{r_\mu} \ll N \forall \mu > 1$, an iterative method yields the self-consistent solution

$$x_1 \approx N - \sum_{\mu=2}^d N^{r_\mu}, \quad x_\mu = N^{r_\mu}, \quad \mu > 1. \quad (8)$$

The dominant transition ratio thus reads

$$\text{DTR} \approx \frac{x_1}{N} \approx 1 - \sum_{\mu=2}^d \frac{1}{N^{1-r_\mu}}, \quad (9)$$

which converges to unity as $N \rightarrow \infty$, with the slowest convergence characterized by the power law $\sim N^{r_2-1}$. Equation (9) provides our first theoretical prediction for ground-state selection. Comparing with numerical simulations of the rate equation (2) for $d = 2$ in Fig. 2(b), the approximate formula (9) agrees qualitatively, with higher accuracy attained for smaller r_2 .

Remarkably, we can solve for the DTR exactly in the asymptotic $N \rightarrow \infty$ limit. In the SM [24], we prove that the dynamics governed by the rate equation (2) is integrable, and derive the complete set of $N + 1$ independent conserved quantities. We thus overcome the problem of nonunique steady states. However, because of the complexity of the exact solution, we only use it to compute the DTR, which reads

$$\text{DTR} = \frac{\bar{n}_1}{N} = 1 - \sum_{\mu=2}^d \frac{\tilde{\Gamma}(1-r_\mu)}{N^{1-r_\mu}}, \quad (10)$$

where $\tilde{\Gamma}(\cdot)$ is the gamma function. The exact solution yields the same scaling as the approximate formula (9), and is in excellent agreement with numerical simulations, as shown in Fig. 2(b). This agreement explains why the approximation of Eq. (9) becomes more accurate for smaller r_μ , since $\tilde{\Gamma}(1-r_\mu) = 1 + O(r_\mu)$. The error in the prefactor of Eq. (9) likely arises from the single-particle approximation.

Our formalism can also be easily extended to include noncollective decay channels, modeled as a leakage at a rate Γ_{leak} [24]. Going back to the fluid model, this adds an extra component $v_0 = \Gamma_{\text{leak}}(N - \sum_{\mu=1}^d x_\mu - x_0)$ to the velocity field and modifies $\sum_{v=1}^d x_v \rightarrow \sum_{v=0}^d x_v$ in Eq. (5). A similar analysis for large N yields $x_0 \approx (\Gamma_{\text{leak}}/\Gamma_1) \ln N$, in the same regime as the validity of Eq. (9). This justifies the omission of noncollective decay in our model, since $x_0 \ll x_\mu \sim N^{r_\mu}$, and the approximate DTR reads

$$\text{DTR} \approx 1 - \sum_{\mu=2}^d \frac{1}{N^{1-r_\mu}} - \frac{\Gamma_{\text{leak}} \ln N}{\Gamma_1 N}. \quad (11)$$

In the noncompeting scenario with only one collective decay channel ($d = 1$), the DTR always converges to unity as $\sim \ln N/N$ (even if $|e\rangle \rightarrow |g_1\rangle$ is not the most dominant transition). This recovers the well-established result of Dicke superradiance in the presence of local decay [15,27]. Moreover, this implies that ground-state selection due to collective decay dominates when $\Gamma_{\text{leak}}/\Gamma_1 \ll N^{r_2}/\ln N$, which is realistic in experimental setups.

The avalanchelike behavior of the dominant transition not only impacts the population of the dominant ground state, but also lowers the fluctuations of the probability distribution dramatically. For $d = 2$, we numerically observe (for small r_2) that the relative fluctuation $\delta n_1/\bar{n}_1$ in the dominant ground-state population vanishes as $N \rightarrow \infty$ faster than $\sim N^{-1/2}$ (expected from independent decay). This causes the steady-state distribution to become sharply peaked at density $n_1/N = 1$, as indicated by the cumulative probability distribution in Fig. 2(c) and in the SM [24]. By the Bhatia-Davis inequality [28], the relative fluctuation can be bounded as $\delta n_1/\bar{n}_1 \leq \sqrt{(1-\text{DTR})/\text{DTR}}$ which vanishes as $\sim N^{(r_2-1)/2}$. While this bound is not tight, it justifies the single-particle approximation made in our theoretical analysis.

Finally, the convergence time T to the steady state can be estimated within the fluid model under the single-particle approximation. By noting that $dt = dx_1/v_1$, we find (see SM [24])

$$T = \frac{1}{\Gamma_1} \int_{\mathcal{C}} \frac{dx_1}{(N - x_1 - \sum_{\mu>1} x_\mu)(x_1 + 1)} \approx \frac{2 - r_2 \ln N}{\Gamma_1 N}, \quad (12)$$

where \mathcal{C} is the trajectory defined by Eq. (7). The presence of competing collective decay channels affects the well-known superradiant timescale of $\Gamma_1 T \sim \ln N/N$ [17] only by a constant factor.

As a possible application of ground-state selection, we analyze the creation of ultracold diatomic molecules via photoassociation. In one-color photoassociation, laser-cooled atoms form weakly bound molecules that spontaneously decay into various more tightly bound states [29]. The vibrational and rotational branching ratios are dictated by Franck-Condon factors and angular-momentum Hönl-London factors, respectively. Specifically, we examine ultracold strontium dimers that lack Feshbach resonances and must be produced optically [30,31]. Strontium dimers have narrow optical transitions and a structureless ground state, making them well suited for metrology [32–35]. We consider photoassociation via the state $(1)1_\mu(v' = -1, J' = 1)$ [33], where v' and J' are the excited-state vibrational and rotational quantum numbers, respectively, and negative vibrational numbers count down from the dissociation threshold. This state has a dominant decay path to the $v = -1, J = 0$ ground state, with an overall branching ratio of $\sim 54\%$ (molecular parameters are detailed in the SM [24]). Our protocol uses a short, strong pulse to create N weakly bound molecules from a dense sample of ultracold atoms. Alternatively, effective decay directly from unbound atoms into ground-state molecules can be engineered via a continuous off-resonant drive [36].

The avalanchelike behavior dramatically enhances the fraction of molecules in the dominant ground state, as shown in Fig. 3. If only one transition is collective, the dominant transition ratio rapidly approaches unity, as shown in Ref. [15]. This can be realized by engineering the dielectric environment to be frequency selective (either via a cavity [37] or a photonic crystal [38]). We note that ground-state selection occurs in the weak-coupling limit of cavity QED, distinguishing it from the so-called ‘‘polaritonic chemistry’’ in strong coupling [39,40]. Figure 3 demonstrates that a nearly pure sample of molecules is created even under maximal competition, where all decay

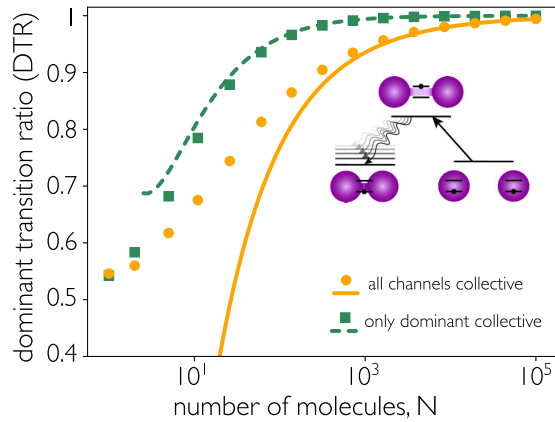


FIG. 3. Targeted photoassociation of a molecular dimer. Weakly bound molecules are created by optical excitation and spontaneously decay to various rovibrational ground-electronic states. The dominant transition ratio (DTR) is plotted against the initial number of weakly bound Sr_2 molecules in the $(1)1_u(\nu' = -1, J' = 1)$ state. Decay is considered to four states, $(\nu = -1, J = 0, 2)$ and $(\nu = -2, J = 0, 2)$ with branching ratios 0.54, 0.27, 0.13, and 0.06, respectively. Points show the numerical solution from the Monte Carlo simulation of the rate equation (2) for the noncompeting scenario where only the dominant transition is collectively enhanced (\square) and the competing scenario with all four collective channels (\circ). The dashed line denotes the analytical prediction (11) for the noncompeting scenario with $\Gamma_{\text{leak}}/\Gamma_1 = 0.852$. The solid line denotes the prediction (10) for the competing scenario. Predictions are valid for $N \gg 1$.

channels are collective. Collective enhancement of all transitions can occur in broadband cavities (or for molecules with a hyperfine structure, which yields smaller frequency differences between levels) or in single-mode fibers [41] within the “mirror configuration” [23]. This effect can also occur in free space with dense, subwavelength molecular clouds. However, in this scenario, collisions can lead to significant losses. For

polar molecules, collisions can be prevented via electric field [42] or microwave shielding [43–46]. Alternatively, they can be suppressed by trapping molecules in optical tweezers to form ordered arrays [47,48]. As these systems are extended, their dynamics are not constrained to the permutationally symmetric subspace. Nevertheless, we expect ground-state selection to occur for molecules placed close to waveguides (at arbitrary distances) or arranged in ordered two- and three-dimensional arrays of subwavelength lattice constant [49,50], albeit with reduced scaling.

In summary, collective decay holds promise for a wide range of quantum systems, from closing open transitions in atoms [12,14] and preventing parasitic decay in solid-state emitters [5,51,52] to directing emission into dielectric nanostructures instead of unwanted modes [20,53]. While we have primarily focused on an initially inverted ensemble, our treatment captures ground-state selection from a large range of multiply excited states. Future research directions include studying the potential for many-body-enhanced metrology [54], due to the sensitivity of the ground-state populations to the decay ratios. Other interesting avenues include the observation of symmetry breaking, which can occur if multiple dominant transitions have identical decay rates, akin to mirror symmetry breaking predicted in waveguide QED [20].

We thank Kon Leung, Luis A. Orozco, and Maximilian Schemmer for helpful discussions. We acknowledge support by the National Science Foundation through the CAREER Award (No. 2047380) and the QLCI program (Grant No. OMA-2016245), the Air Force Office of Scientific Research through their Young Investigator Prize (Grant No. 21RT0751) and through Grant No. FA9550-1910328, ARO through the MURI program (Grant No. W911NF-20-1-0136), DARPA (Grant No. W911NF2010090), as well as by the David and Lucile Packard Foundation and the Brown Science Foundation. The Institute for Quantum Information and Matter is an NSF Physics Frontiers Center.

- [1] I. Cong, H. Levine, A. Keesling, D. Bluvstein, S.-T. Wang, and M. D. Lukin, Hardware-efficient, fault-tolerant quantum computation with Rydberg atoms, *Phys. Rev. X* **12**, 021049 (2022).
- [2] L. D. Carr, D. DeMille, R. V. Krems, and J. Ye, Cold and ultracold molecules: Science, technology and applications, *New J. Phys.* **11**, 055049 (2009).
- [3] J. L. Bohn, A. M. Rey, and J. Ye, Cold molecules: Progress in quantum engineering of chemistry and quantum matter, *Science* **357**, 1002 (2017).
- [4] M. Atatüre, D. Englund, N. Vamivakas, S.-Y. Lee, and J. Wrachtrup, Material platforms for spin-based photonic quantum technologies, *Nat. Rev. Mater.* **3**, 38 (2018).
- [5] C. M. Lange, E. Daggett, V. Walther, L. Huang, and J. D. Hood, Superradiant and subradiant states in lifetime-limited organic molecules through laser-induced tuning, *Nat. Phys.* **20**, 836 (2024).
- [6] H. Walther, B. T. H. Varcoe, B.-G. Englert, and T. Becker, Cavity quantum electrodynamics, *Rep. Prog. Phys.* **69**, 1325 (2006).
- [7] E. Vetsch, D. Reitz, G. Sagué, R. Schmidt, S. T. Dawkins, and A. Rauschenbeutel, Optical interface created by laser-cooled atoms trapped in the evanescent field surrounding an optical nanofiber, *Phys. Rev. Lett.* **104**, 203603 (2010).
- [8] P. Solano, P. Barberis-Blostein, F. K. Fatemi, L. A. Orozco, and S. L. Rolston, Super-radiance reveals infinite-range dipole interactions through a nanofiber, *Nat. Commun.* **8**, 1857 (2017).
- [9] A. Goban, C.-L. Hung, J. D. Hood, S.-P. Yu, J. A. Muniz, O. Painter, and H. J. Kimble, Superradiance for atoms trapped along a photonic crystal waveguide, *Phys. Rev. Lett.* **115**, 063601 (2015).
- [10] X. Zhou, H. Tamura, T.-H. Chang, and C.-L. Hung, Trapped atoms and superradiance on an integrated nanophotonic microring circuit, *Phys. Rev. X* **14**, 031004 (2024).

- [11] W. A. Molander and C. R. Stroud, Jr., Altered branching ratios and relaxation oscillations in superfluorescent cascades, *J. Phys. B: At. Mol. Phys.* **15**, 2109 (1982).
- [12] R. T. Sutherland and F. Robicheaux, Superradiance in inverted multilevel atomic clouds, *Phys. Rev. A* **95**, 033839 (2017).
- [13] A. Piñeiro Orioli, J. K. Thompson, and A. M. Rey, Emergent dark states from superradiant dynamics in multilevel atoms in a cavity, *Phys. Rev. X* **12**, 011054 (2022).
- [14] S. J. Masson, J. P. Covey, S. Will, and A. Asenjo-Garcia, Dicke superradiance in ordered arrays of multilevel atoms, *PRX Quantum* **5**, 010344 (2024).
- [15] D. Wellnitz, S. Schütz, S. Whitlock, J. Schachenmayer, and G. Pupillo, Collective dissipative molecule formation in a cavity, *Phys. Rev. Lett.* **125**, 193201 (2020).
- [16] R. H. Dicke, Coherence in spontaneous radiation processes, *Phys. Rev.* **93**, 99 (1954).
- [17] M. Gross and S. Haroche, Superradiance: An essay on the theory of collective spontaneous emission, *Phys. Rep.* **93**, 301 (1982).
- [18] J. P. Clemens, L. Horvath, B. C. Sanders, and H. J. Carmichael, Shot-to-shot fluctuations in the directed superradiant emission from extended atomic samples, *J. Opt. B: Quantum Semiclass. Opt.* **6**, S736 (2004).
- [19] S. J. Masson and A. Asenjo-Garcia, Universality of Dicke superradiance in arrays of quantum emitters, *Nat. Commun.* **13**, 2285 (2022).
- [20] S. Cardenas-Lopez, S. J. Masson, Z. Zager, and A. Asenjo-Garcia, Many-body superradiance and dynamical mirror symmetry breaking in waveguide QED, *Phys. Rev. Lett.* **131**, 033605 (2023).
- [21] N. J. Fitch and M. R. Tarbutt, Laser-cooled molecules, *Adv. At., Mol., Opt. Phys.* **70**, 157 (2021).
- [22] D. E. Chang, L. Jiang, A. V. Gorshkov, and H. J. Kimble, Cavity QED with atomic mirrors, *New J. Phys.* **14**, 063003 (2012).
- [23] H. L. Sørensen, J.-B. Béguin, K. W. Kluge, I. Iakoupov, A. S. Sørensen, J. H. Müller, E. S. Polzik, and J. Appel, Coherent backscattering of light off one-dimensional atomic strings, *Phys. Rev. Lett.* **117**, 133604 (2016).
- [24] See Supplemental Material at <http://link.aps.org/supplemental/10.1103/PhysRevResearch.7.L022015> for additional calculation details, which includes Refs. [55–59].
- [25] V. Degiorgio and F. Ghielmetti, Approximate solution to the superradiance master equation, *Phys. Rev. A* **4**, 2415 (1971).
- [26] C. M. Bender and S. A. Orszag, Perturbation series, in *Advanced Mathematical Methods for Scientists and Engineers I: Asymptotic Methods and Perturbation Theory* (Springer, New York, 1999), pp. 319–367.
- [27] D. Malz, R. Trivedi, and J. I. Cirac, Large- N limit of Dicke superradiance, *Phys. Rev. A* **106**, 013716 (2022).
- [28] R. Bhatia and C. Davis, A better bound on the variance, *Am. Math. Mon.* **107**, 353 (2000).
- [29] K. M. Jones, E. Tiesinga, P. D. Lett, and P. S. Julienne, Ultracold photoassociation spectroscopy: Long-range molecules and atomic scattering, *Rev. Mod. Phys.* **78**, 483 (2006).
- [30] S. Stellmer, B. Pasquiou, R. Grimm, and F. Schreck, Creation of ultracold Sr₂ molecules in the electronic ground state, *Phys. Rev. Lett.* **109**, 115302 (2012).
- [31] G. Reinaudi, C. B. Osborn, M. McDonald, S. Kotochigova, and T. Zelevinsky, Optical production of stable ultracold ⁸⁸Sr₂ molecules, *Phys. Rev. Lett.* **109**, 115303 (2012).
- [32] T. Zelevinsky, S. Kotochigova, and J. Ye, Precision test of mass-ratio variations with lattice-confined ultracold molecules, *Phys. Rev. Lett.* **100**, 043201 (2008).
- [33] K. H. Leung, B. Iritani, E. Tiberi, I. Majewska, M. Borkowski, R. Moszynski, and T. Zelevinsky, Terahertz vibrational molecular clock with systematic uncertainty at the 10⁻¹⁴ level, *Phys. Rev. X* **13**, 011047 (2023).
- [34] S. S. Kondov, C.-H. Lee, K. H. Leung, C. Liedl, I. Majewska, R. Moszynski, and T. Zelevinsky, Molecular lattice clock with long vibrational coherence, *Nat. Phys.* **15**, 1118 (2019).
- [35] E. Tiberi, M. Borkowski, B. Iritani, R. Moszynski, and T. Zelevinsky, Searching for new fundamental interactions via isotopic shifts in molecular lattice clocks, *Phys. Rev. Res.* **6**, 033013 (2024).
- [36] S. Inouye, A. P. Chikkatur, D. M. Stamper-Kurn, J. Stenger, D. E. Pritchard, and W. Ketterle, Superradiant Rayleigh scattering from a Bose-Einstein condensate, *Science* **285**, 571 (1999).
- [37] T. Kampschulte and J. H. Denschlag, Cavity-controlled formation of ultracold molecules, *New J. Phys.* **20**, 123015 (2018).
- [38] J. Pérez-Ríos, M. E. Kim, and C.-L. Hung, Ultracold molecule assembly with photonic crystals, *New J. Phys.* **19**, 123035 (2017).
- [39] J. Feist, J. Galego, and F. J. Garcia-Vidal, Polaritonic chemistry with organic molecules, *ACS Photonics* **5**, 205 (2018).
- [40] M. Hertzog, M. Wang, J. Mony, and K. Börjesson, Strong light-matter interactions: A new direction within chemistry, *Chem. Soc. Rev.* **48**, 937 (2019).
- [41] M. Márquez-Mijares, B. Lepetit, and E. Brion, Nanofibre-based trap for Rb₂ molecule, *Phys. Scr.* **98**, 115404 (2023).
- [42] G. Valtolina, K. Matsuda, W. G. Tobias, J.-R. Li, L. De Marco, and J. Ye, Dipolar evaporation of reactive molecules to below the Fermi temperature, *Nature (London)* **588**, 239 (2020).
- [43] L. Anderegg, S. Burchesky, Y. Bao, S. S. Yu, T. Karman, E. Chae, K.-K. Ni, W. Ketterle, and J. M. Doyle, Observation of microwave shielding of ultracold molecules, *Science* **373**, 779 (2021).
- [44] A. Schindewolf, R. Bause, X.-Y. Chen, M. Duda, T. Karman, I. Bloch, and X.-Y. Luo, Evaporation of microwave-shielded polar molecules to quantum degeneracy, *Nature (London)* **607**, 677 (2022).
- [45] J. Lin, G. Chen, M. Jin, Z. Shi, F. Deng, W. Zhang, G. Quémener, T. Shi, S. Yi, and D. Wang, Microwave shielding of bosonic NaRb molecules, *Phys. Rev. X* **13**, 031032 (2023).
- [46] N. Bigagli, W. Yuan, S. Zhang, B. Bulatovic, T. Karman, I. Stevenson, and S. Will, Observation of Bose-Einstein condensation of dipolar molecules, *Nature (London)* **631**, 289 (2024).
- [47] L. Anderegg, L. W. Cheuk, Y. Bao, S. Burchesky, W. Ketterle, K.-K. Ni, and J. M. Doyle, An optical tweezer array of ultracold molecules, *Science* **365**, 1156 (2019).
- [48] C. M. Holland, Y. Lu, and L. W. Cheuk, On-demand entanglement of molecules in a reconfigurable optical tweezer array, *Science* **382**, 1143 (2023).
- [49] E. Sierra, S. J. Masson, and A. Asenjo-Garcia, Dicke superradiance in ordered lattices: Dimensionality matters, *Phys. Rev. Res.* **4**, 023207 (2022).
- [50] W.-K. Mok, A. Poddar, E. Sierra, C. C. Rusconi, J. Preskill, and A. Asenjo-Garcia, Universal scaling laws for correlated decay of many-body quantum systems, [arXiv:2406.00722](https://arxiv.org/abs/2406.00722).
- [51] A. Sipahigil, R. E. Evans, D. D. Sukachev, M. J. Burek, J. Borregaard, M. K. Bhaskar, C. T. Nguyen, J. L. Pacheco, H. A.

- Atikian, C. Meuwly, R. M. Camacho, F. Jelezko, E. Bielejec, H. Park, M. Lončar, and M. D. Lukin, An integrated diamond nanophotonics platform for quantum-optical networks, *Science* **354**, 847 (2016).
- [52] M. Scheibner, T. Schmidt, L. Worschech, A. Forchel, G. Bacher, T. Passow, and D. Hommel, Superradiance of quantum dots, *Nat. Phys.* **3**, 106 (2007).
- [53] C. Liedl, F. Tebbenjohanns, C. Bach, S. Pucher, A. Rauschenbeutel, and P. Schneeweiss, Observation of superradiant bursts in a cascaded quantum system, *Phys. Rev. X* **14**, 011020 (2024).
- [54] D.-S. Ding, Z.-K. Liu, B.-S. Shi, G.-C. Guo, K. Mølmer, and C. S. Adams, Enhanced metrology at the critical point of a many-body Rydberg atomic system, *Nat. Phys.* **18**, 1447 (2022).
- [55] N. Shammah, S. Ahmed, N. Lambert, S. De Liberato, and F. Nori, Open quantum systems with local and collective incoherent processes: Efficient numerical simulations using permutational invariance, *Phys. Rev. A* **98**, 063815 (2018).
- [56] K. H. Leung, The strontium molecular lattice clock: Vibrational spectroscopy with hertz-level accuracy, Ph.D. thesis, Columbia University, 2023.
- [57] M. Borkowski (private communication).
- [58] I. Majewska, Theoretical description of ultracold strontium molecules in an optical lattice: Control of photodissociation and interpretation of molecular clock experiments, Ph.D. thesis, University of Warsaw, 2021.
- [59] T. Zelevinsky, M. M. Boyd, A. D. Ludlow, T. Ido, J. Ye, R. Ciuryło, P. Naidon, and P. S. Julienne, Narrow line photoassociation in an optical lattice, *Phys. Rev. Lett.* **96**, 203201 (2006).